

Article

Experimental Investigation to Evaluate the Dynamic Properties of a Scaled Rectangular Tuned Liquid Damper Using High-Speed Videos

Rigoberto Nava-González, Adrián Pozos-Estrada * , Roberto Gómez-Martínez and Oscar Pozos-Estrada

Institute of Engineering, National Autonomous University of Mexico, Mexico City 04510, Mexico; rnavag@iingen.unam.mx (R.N.-G.); rgomez@iingen.unam.mx (R.G.-M.); opozose@iingen.unam.mx (O.P.-E.)

* Correspondence: apozose@iingen.unam.mx

Abstract: The use of tuned liquid dampers (TLDs) as an alternative to reduce the response of flexible structures with a low amount of structural damping is a viable option. The correct characterization of the dynamic properties of the TLD plays an important role in the performance of the TLD-main structure system. This work presents the results of an experimental study to evaluate the dynamic properties of a scaled rectangular TLD using high-speed videos. For the experimental investigation, a scaled rectangular TLD is subjected to lateral displacement of the sinusoidal type with amplitudes that range from 5 to 40 mm and frequency equal to 0.625 Hz. The dynamic properties of the TLD system are identified with the use of high-speed videos with a duration of 28.96 s and recorded at 500 frames per second (fps). The recorded videos are analyzed with the software Tracker to extract time histories of wave elevation at predefined locations. The frequency and damping of the TLD system are identified from the time histories of wave elevation through Fourier analysis and free-vibration decay. The findings of this study revealed that the identified dynamic properties of the TLD by using high-speed videos presented small differences with respect to the target values, with errors that range from 0.93 to 2.9% for frequency and from 1.6 to 8.8% for damping, indicating that the use of high-speed videos can be an alternative to evaluate the dynamic properties of TLD systems.



Citation: Nava-González, R.; Pozos-Estrada, A.; Gómez-Martínez, R.; Pozos-Estrada, O. Experimental Investigation to Evaluate the Dynamic Properties of a Scaled Rectangular Tuned Liquid Damper Using High-Speed Videos. *Buildings* **2024**, *14*, 331. <https://doi.org/10.3390/buildings14020331>

Academic Editor: Pedro Martinez-Vazquez

Received: 22 December 2023

Revised: 12 January 2024

Accepted: 22 January 2024

Published: 24 January 2024



Copyright: © 2024 by the authors. Licensee MDPI, Basel, Switzerland. This article is an open access article distributed under the terms and conditions of the Creative Commons Attribution (CC BY) license (<https://creativecommons.org/licenses/by/4.0/>).

Keywords: tuned liquid damper; damping; modal frequency; experimental testing; high-speed video

1. Introduction

The use of energy dissipation devices to reduce the structural response under wind or seismic forces has been investigated by different authors [1–3], and their performance for wind and earthquake-induced responses are considered to be satisfactory. One of the passive energy dissipation systems is the tuned liquid damper (TLD). The use of TLDs as vibration reduction devices in civil structures started around the 1970s in offshore structures, by showing the effects of installing storage tanks and observing how the variation of the water flow directly influences both the water frequency and its damping [4]. In the 1980s, a study of the influence of appendages applied as an equivalent mechanical model attached to a system of multiple degrees of freedom was carried out, such a study showed that the response of the primary system was reduced when one of the sloshing modes of the appendages is tuned to the fundamental mode of the primary structure [5]. The application of TLDs in tall structures began in Japan with the installation of TLDs in two control towers, an observatory tower, and finally a high-rise building. In these structures, the behavior of the system without and with the TLD was measured, and the results were quite good to be able to observe the reduction of their responses with the use of the TLDs [6].

More recently, methodologies for modeling and design of the TLD system have been developed [3]. Other investigations have studied the non-linear component of the liquid breaking against interior dissipative elements (e.g., screens), and some variants of a TLD system have been developed as well [7–10]. Another proposal is to use hybrid systems in

conjunction with base isolators, which initially brings the structure to a higher period, and in turn translates into lower frequencies at which the TLD device is effectively activated, resulting in improved building performance [11].

A traditional TLD device consists of a partially filled container, usually of rectangular shape with length (L), width (b), and quiescent fluid depth (h). The TLD is rigidly connected to the main structure. The sloshing frequency of the TLD device is tuned near to the modal frequency of the structure. The optimal properties of the TLD are usually obtained by parametric analysis [12]; the parametric analysis considers adjustments in L , b , and h .

The TLD is an attractive technology due to its low cost, easy installation, and maintenance, as well as its ability to absorb energy since the device dissipates structural energy through the sloshing of the liquid as it breaks against the walls of the TLD [13]. Inherent damping can be increased by installing dissipative devices, such as screens, nets, floating bases, baffles, and other elements [14–18].

The main parameters that characterize the design of a TLD system can be defined as the mass ratio, μ , frequency ratio, Ω , and damping ratio, Φ . For a given structure, the optimal TLD system is often defined as the one that generates the minimum structural response. It is noted that a practical methodology to calculate the optimal parameters of the TLDs, based on equivalent TLD properties, has been proposed by [12]. This methodology has also been used by [19] to develop a preliminary design method for TLDs conforming to space restrictions. More recently, a practical performance-based design approach was developed by [20] which is based on the work by [12]. In this study, the methodology proposed by [12] is adopted to calculate the optimal parameters of the TLDs. The successful implementation of an auxiliary damping device, such as the TLD, includes a correct characterization of its dynamic properties.

The use of nonintrusive methodologies to evaluate the properties of dynamic systems has gained much attention in recent years. For example [21] employed image-recognition techniques to monitor the dynamic response of small-scale structures, [22] used a flow visualization technique and a high-speed camera to estimate air concentration profiles for a series of hydraulic jumps. Other examples of the use of nonintrusive methodologies that include the use of videos recorded with high-speed cameras are those presented by Gardarsson [23]. In Gardarsson's study, laser imaging to measure the sloshing behavior of a water tank using shaking table tests was used. Lobovský et al. [24] carried out investigations of the behavior of dynamic pressures during dam failure using a high-speed video camera. Min et al. [25] developed a fast vision detection system based on the binary pixel count of the image portion in a pseudo-dynamic test of a Tuned Liquid Column Damper (TLCD). Poguluri and Cho [26] used high-speed videos to compare the sloshing behavior of a rectangular tank with the results obtained from numerical analysis based on computational fluid dynamics (CFD). More recently, experimental investigations have been developed in which the performance of structures equipped with TLDs has been measured using high-definition videos to verify the response of both the main system and the auxiliary device [27,28]. The previous studies provided a forward step towards the understanding of the use of high-speed cameras to study dynamic systems; however, the use of high-speed videos to identify dynamic properties of TLDs in dynamic tests has not been reported in the literature.

The main objective of this study is to evaluate the dynamic properties (i.e., frequency and damping ratio) of a scaled rectangular TLD using high-speed videos. For the experimental setup, the TLD model is subjected to lateral displacement demands with amplitudes that range from 5 to 40 mm. A dynamic actuator is used to apply the lateral displacement. High-speed videos of water elevation at selected points are recorded with a high-speed camera attached to the experimental device. The software Tracker Version 6.1.3 is employed to extract time histories of wave elevation at predefined locations. Fourier analysis and free-vibration decay of the wave elevation records are carried out to identify the dynamic properties of the TLD.

2. Experimental Setup

2.1. General

The design of the TLD requires the definition of μ , Ω , and Φ . To evaluate such parameters, the dynamic properties of a previously studied tall building [29] were used. The building properties that were taken as the basis for the TLD design were a modal mass value associated with the first mode of vibration equal to 7.673×10^6 (kg), a structural damping ratio equal to 1%, and a modal frequency equal to 0.199 Hz [29]. To calculate the model parameters, the scaling factors shown in Table 1 were employed. The building was equipped with a TLD device located at the top. The conceptual design of the TLD is based on research on an equivalent linear mechanical model proposed by [12], where potential flow theory is used to describe the behavior of a TLD equipped with damping screens. By applying the aforementioned methodology, the optimal dimensions of the tank were obtained and are equal to $L = 10$ m, $b = 10$ m, and $h = 1.75$ m. To verify that the calculated properties of the TLD device are consistent with the performance of the physical model, a series of experimental tests were carried out.

Table 1. Similarity scales for the TLD model.

Scales	Definitions	Target Values	Values
Length	$\lambda_L = L_m/L_p$	1/10	0.10
Density	$\lambda_\rho = \rho_m/\rho_p$	1/1	1
Time	$\lambda_T = (\lambda_L)^{1/2}$	$(1/10)^{1/2}$	0.316
Frequency	$\lambda_f = 1/\lambda_T$	$1/(1/10)^{1/2}$	3.16
Acceleration	$\lambda_a = \lambda_L (\lambda_T)^{-2}$	1	1
Damping	$\xi_L = \xi_m/\xi_p$	1/1	1
Mass	$\lambda_M = \lambda_L^3$	$(1/10)^3$	0.001
Force	$\lambda_F = \lambda_L^3$	$(1/10)^3$	0.001

The experimental test specimen, developed at the laboratory of structures and materials of the Institute of Engineering of the National Autonomous University of México, consists of a scaled model of the TLD capable of replicating the dynamic properties of the full-scale prototype. The TLD is mounted on a steel frame that is excited by an MTS 244.22 actuator (MTS Systems, Eden Prairie, MN, USA) in a uni-directional manner. Figure 1 shows the general setup of the experimental test.

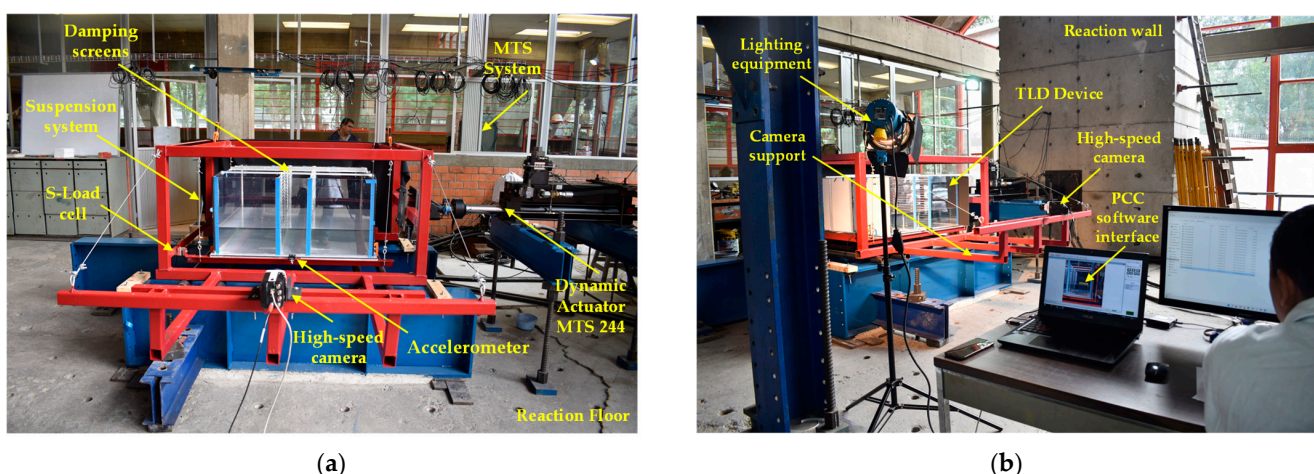


Figure 1. Experimental setup: (a) Preparation for the test; (b) lighting equipment and test execution.

The analytical solution predicts the peaks near the lowest theoretical resonance frequencies, which are obtained according to Equation (1) [30]. The natural frequencies, f_{TLD} , for the n th sloshing modes in a rectangular tank can be calculated based on L and h . The parameter g is the universal constant of gravity equal to 9.81 m/s².

$$f_{TLD} = \frac{1}{2\pi} \sqrt{\frac{n\pi g}{L} \tanh\left(\frac{n\pi h}{L}\right)} \quad (1)$$

Considering the scaling relationships and Equation (1), the first 3 natural frequencies for the rectangular tank are equal to 0.625 Hz (1.60 s), 1.12 Hz (0.89 s), and 1.47 Hz (0.7 s). In the case of damping, equations have been presented in the literature that allow estimating the supplementary damping provided by a TLD system when dissipative screens are placed. In the present investigation, it is assumed that for sinusoidal excitation, Equation (2) can be used to determine the equivalent damping ratio depending on the amplitude of excitation [12]:

$$\zeta_{eq} = C_I \frac{16}{3\pi^2} \tanh^2\left(\frac{\pi h}{L}\right) \Delta \bar{\Xi} \frac{x_r}{L} \quad (2)$$

where C_I is a loss coefficient, $\Delta \bar{\Xi}$ is a parameter that relates the damping to the screen position in the tank for the fundamental sloshing mode, and x_r is the distance between the screens.

2.2. Tank

The rectangular tank was built with transparent acrylic to allow visual observation of the liquid movement and wave elevation change at the interface of the tank walls. The acrylic plates were glued and sealed with polyurethane silicone. The tank is 1000 mm long, 500 mm high, and 1000 mm wide. The thickness of the acrylic is 9.5 mm. The tank has 2 dissipative screens placed at $0.4L$ and $0.6L$, which allow a solidity ratio of 0.42, the dissipative screens are made of $1/2'' \times 1/8''$ thick aluminum sill, and at a vertical spacing equidistant of 10 mm to complete the 500 mm height. Figure 2 shows the dimensions of the tank and screen, as well as pictures of the tank and screens.

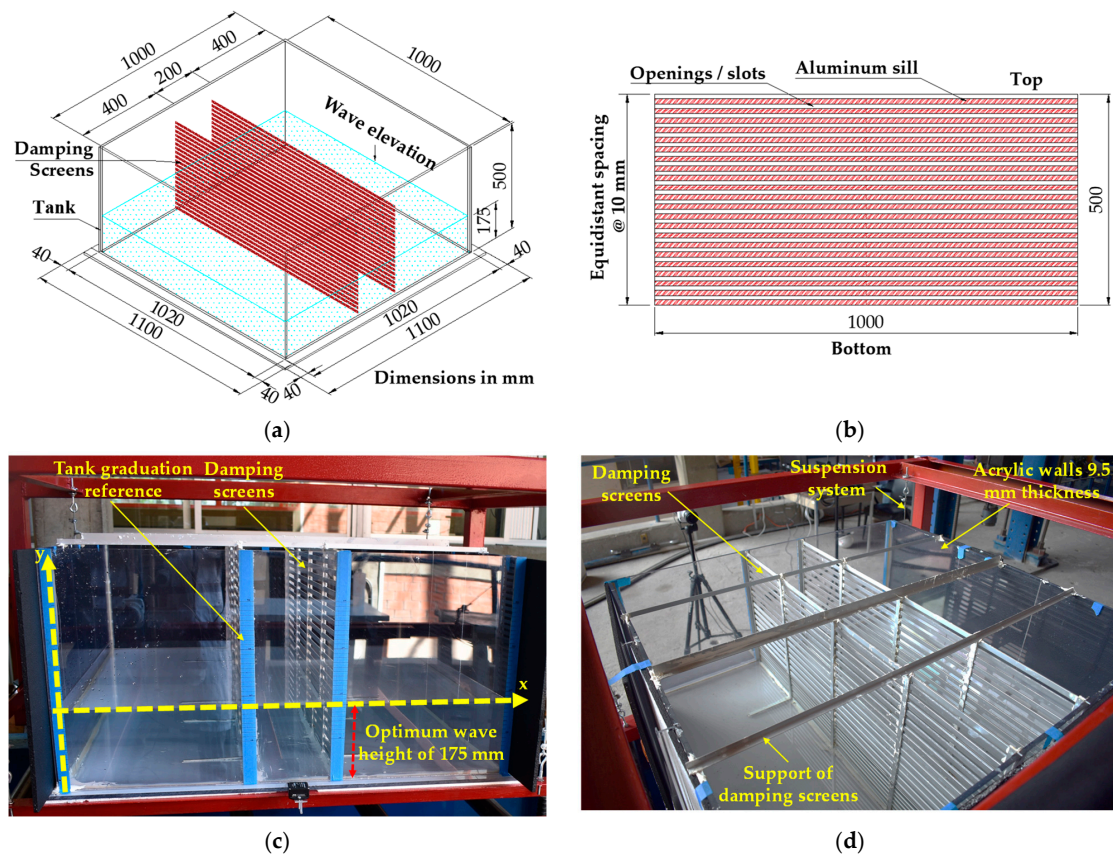


Figure 2. Tank design: (a) Dimensions of the TLD model; (b) geometrical details of the slotted screen; (c) TLD model with damping screens; (d) view of the damping screens.

2.3. Test Protocol

The dynamic response of a TLD depends directly on the arrangement of the dissipative screens, as well as on the behavior of the liquid under lateral loading. The loading protocol used for the evaluation of the dynamic properties of the TLD system (i.e., damping, ζ_{TLD} , and frequency of the contained liquid, f_{w-exp}) is based on that proposed by [31], which considers sinusoidal excitation with different amplitudes and a frequency, f . For the experimental tests, the parameter β_w is defined as the ratio between the excitation frequency, f , and the fundamental sloshing frequency, f_w .

Based on the dynamic properties of the tall building considered, and the similarity scales presented in Table 1, the frequency value of the input signal was set equal to 0.625 Hz. Table 2 shows the values of the amplitudes used to characterize the sinusoidal excitation in the experimental tests; it is worth mentioning that the variation of the amplitudes is due to the fact that the aim was to verify that the behavior of the dynamic properties of the system is maintained regardless the magnitude of the amplitude.

Table 2. Test parameters of the TLD model.

Excitation Amplitude A , mm	Frequency Ratio $\beta_w = f/f_w$	Number Tests
40	1	5
20	1	5
15	1	5
10	1	5
5	1	5

Since the frequency of the input signals had to comply with the required β_w during the experimental tests, it was decided to perform signal tuning, which consists of equalizing in terms of amplitude and minimizing the deviation that occurs for each time step between the input and output signals of the MTS 244.22 actuator. A comparison of the actuator input signal versus the actuator motion signal is presented in Figure 3. It can be observed in Figure 3 that the signal has a 10 s delay with respect to the start of the input signal since a 10 s zero offset ramp was added to have better control of the measured data. Also, it is observed that the signals practically overlap. During tuning, the percentage of error between the displacement executed by the actuator and the displacement sensor (LVDT) was about 0.02%.

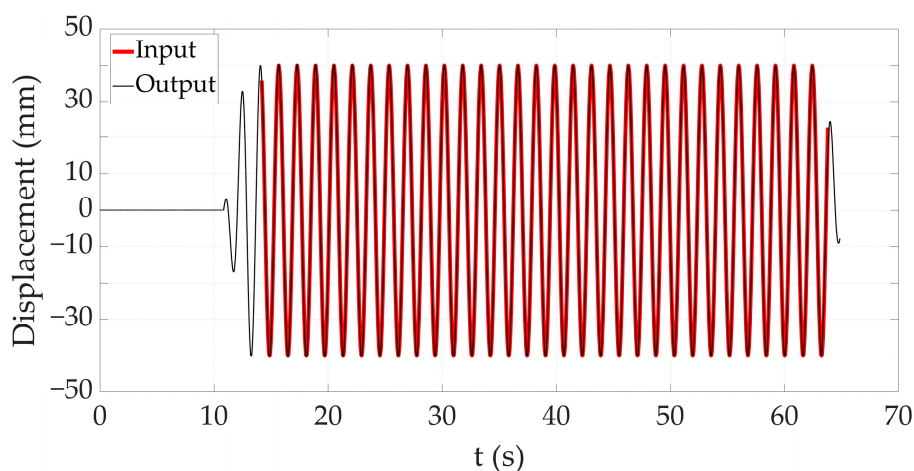


Figure 3. Comparison of the input and output signals of the actuator during tuning.

3. System Identification

System identification methodologies are applied to obtain the dynamic parameters of the TLD tuned to the reference parameters of the building. These parameters are identified for the system separately, as described in the following sections.

3.1. Data Acquisition with High-Speed Videos

The use of non-intrusive techniques in the characterization of the dynamic response of mechanical systems has been advancing over the years. The use of high-speed videos is a viable option for this purpose, as high-speed cameras have sampling rates in excess of 100 frames per second (fps). The use of high-speed video allows capturing the behavior of highly-sampling rate-dependent systems such as TLD systems, or other types of systems that operate at high speeds and that are normally difficult to perceive by the human eye.

During the experiments, a high-speed camera was used to record during the tests at a rate of 500 fps, with a duration of 28.96 s, a lighting system was used to improve the light in the videos. The evolution of the free surface and the impact of water with the dissipative screens placed at $0.4L$ and $0.6L$ were recorded. Lateral views were considered from 3 different positions of the camera, two at the ends to capture the evolution of the flow in the control boxes, and one at the center of the tank to capture the behavior of the flow when breaking against the screens. Figure 4a shows the control zones for tracking the free surface, as well as the position points of the high-speed camera. Figure 4b shows a picture of the evolution of the free surface under sinusoidal loading.

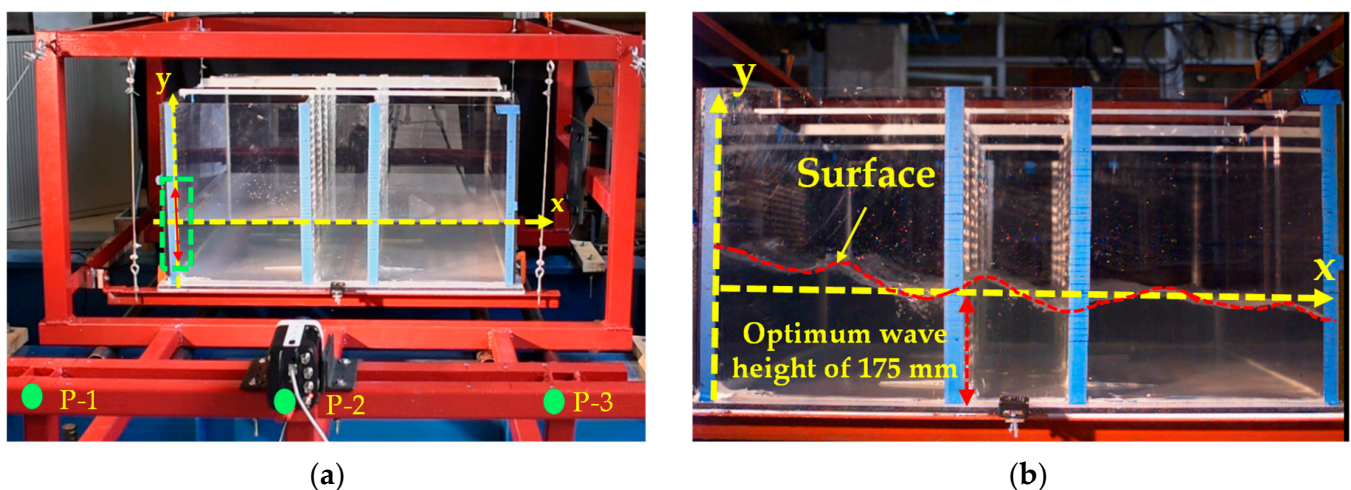


Figure 4. TLD during the tests: (a) Surface of the liquid at the reference height and control box (green box) to be recorded during the experiment; (b) liquid surface movement due to the sloshing component.

The postprocessing of the high-speed videos was carried out with the program Tracker [32], which is a free program built with Java Version 8 (Open-Source Physics) for modeling and analysis. Tracker is based on the recognition of points in a 2D space, by associating a mass or control node to be monitored, making it possible to obtain time histories of wave elevation, velocities, or accelerations at predefined points.

The methodology used to extract time histories of wave elevation by using the program Tracker included the following steps:

- (1) To import the videos previously recorded with the high-speed camera in .mov format;
- (2) To calibrate and add a rod in Tracker, which consists of assigning a standard measurement in the working area (for the case of the experimental tests of the present work it was taken as 175 mm, level of water in rest);

- (3) To declare the point of origin from which Tracker is going to generate the values of the position of the control box;
- (4) To create the mass point, which consists of creating a control frame that will be tracked with the auto-tracker. For this point, if the previous steps were performed carefully, the auto-tracker will generate data vectors that represent time histories of displacement for the horizontal and vertical components at the selected point;
- (5) To export the obtained time histories of wave elevation to an Excel file or .txt file for further processing.

Figure 5 shows the Tracker interface with the selected point to be tracked in an XY plane, in the right-hand side of the figure the time histories of vertical and horizontal displacements are shown. For all the analyses, only the time histories of the vertical displacement (wave elevation) were used.

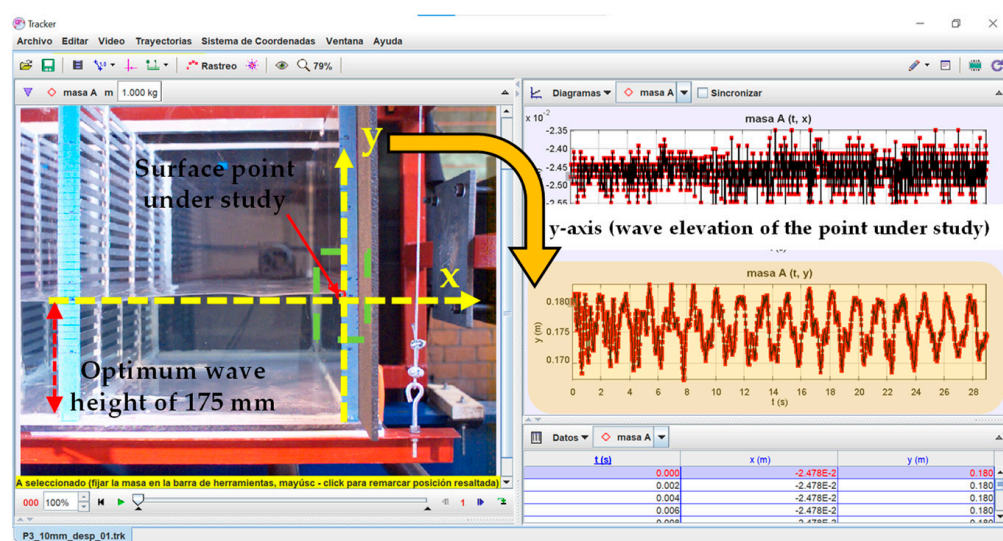


Figure 5. Tracker Software interface.

3.2. Dynamic Properties

To analyze the time histories of wave elevation obtained with the software Tracker, and to obtain the experimental frequency of the TLD, the Fast Fourier Transform (FFT) and Wavelet Transform were used. The inherent damping ratio of the TLD system was obtained using the free-vibration decay methodology [33]. Figure 6 shows the flowchart employed to identify the dynamic properties of the TLD system. It is observed in Figure 6 that the flowchart starts with the recording of the high-speed video for subsequent processing with the program Tracker to define the time histories of wave elevation.

During the Fourier analysis process, the Fourier amplitude spectra of all the wave elevation signals were calculated. Based on the actual Fourier amplitude spectra, some low- and high-frequency noise were observed. To remove the noise from the original data, a bandpass filter with corner frequencies equal to 0.59 and 0.65 Hz is applied. These corner frequencies are close to the target frequency. The dominant frequency in the amplitude spectra of the filtered signals is identified. Finally, a free-vibration decay methodology is employed to obtain the damping properties.

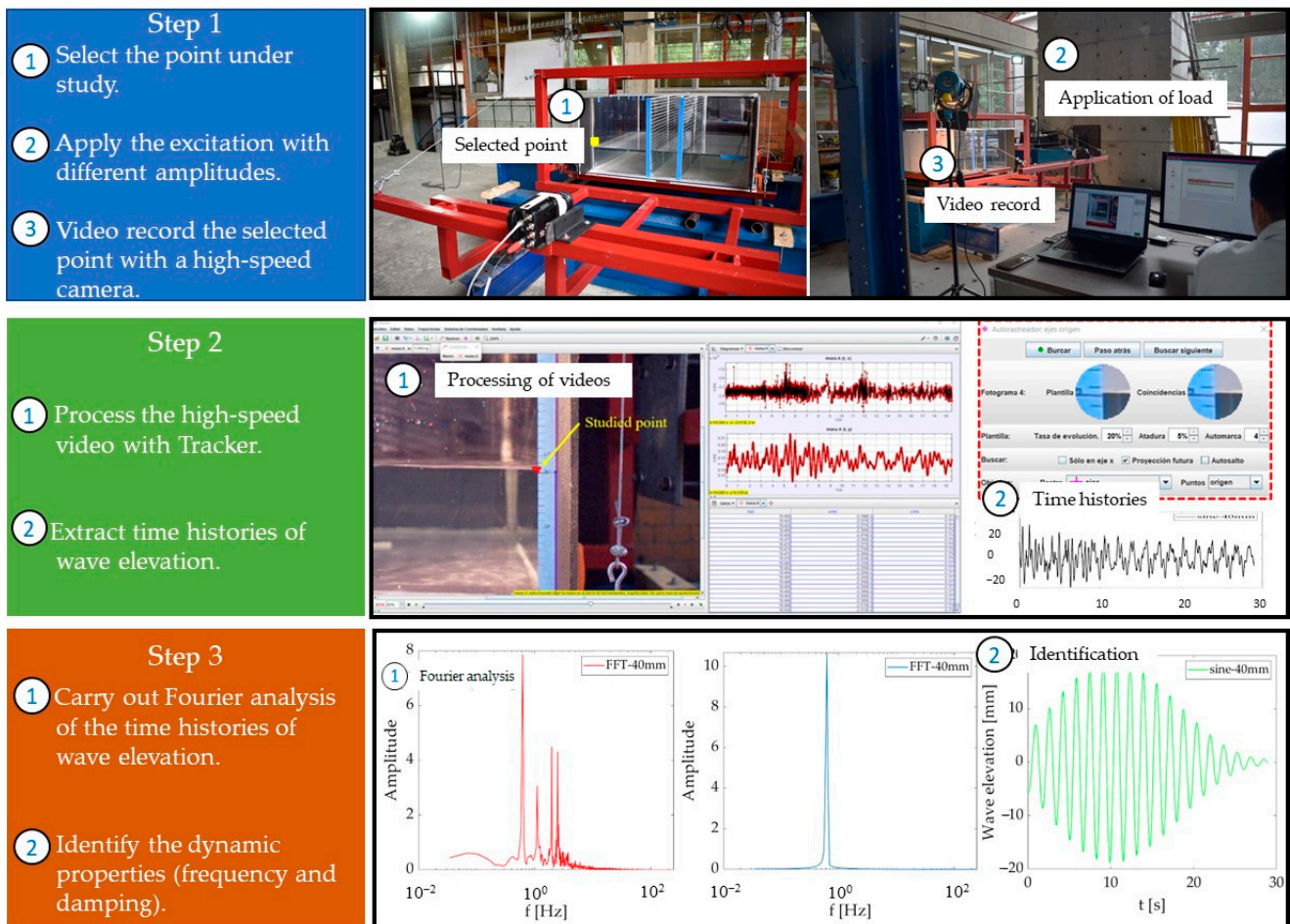


Figure 6. Flowchart for the characterization of dynamic properties of the TLD system, using high-speed videos.

4. Results

Sine functions characterized by the amplitudes presented in Table 2 were used to represent the lateral demand on the TLD system. In all cases, the frequency of the excitation was fixed at 0.625 Hz. Figure 7a–e shows time histories (with and without bandpass filter) of wave elevation at the surface point when the camera was located at position P-1. It is noted that the selected filter affects the original signal, which is expected, as the bandpass filter removes the energy content associated with low- and high-frequency noise, except in the bandpass employed. It is worth mentioning that during the Fourier synthesis, only the energy content within the bandpass was employed. Also in Figure 7f, the spectra of Fourier amplitudes of the time histories of wave elevation are presented. The horizontal axis of Figure 7f is presented in terms of the β_w value. It is observed in Figure 7f that the peaks of the spectra are located around $\beta_w = 1$, which indicates that the identified frequency is very similar to the target frequency (i.e., 0.625 Hz).

To further evaluate the identified frequency of the TLD system, Figure 8 shows the wavelet scalogram of the original time histories of wave elevation (i.e., without band-pass filter). It is observed in Figure 8 that the energy in the signals is concentrated very close to the target frequency (0.625 Hz). In Figure 8, other frequencies can be observed with a certain amount of energy that can be associated with higher frequencies of the TLD system.

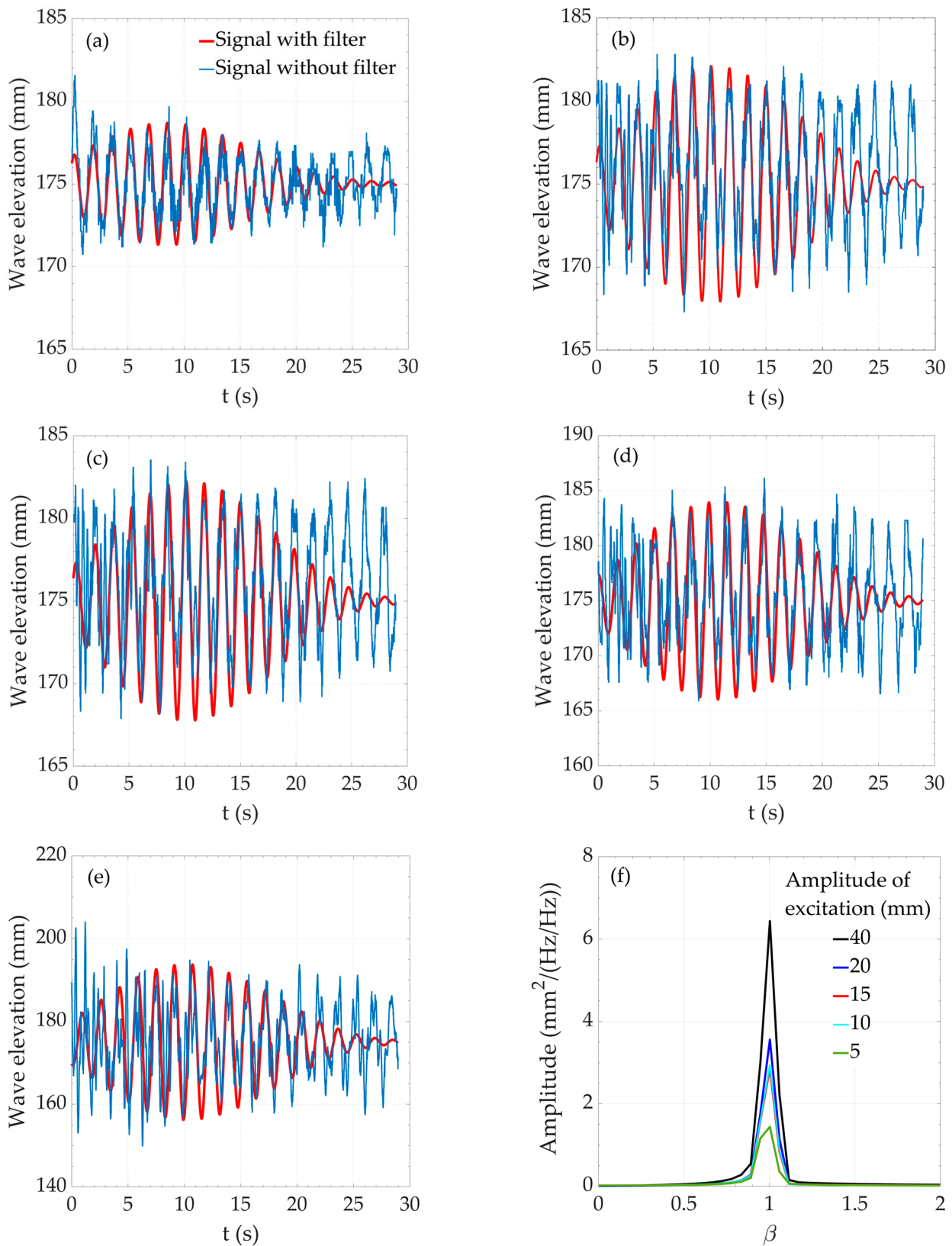


Figure 7. Time histories of experimental wave elevation with and without band-pass filter: (a) 5 mm amplitude sinusoidal excitation; (b) 10 mm amplitude sinusoidal excitation; (c) 15 mm amplitude sinusoidal excitation; (d) 20 mm amplitude sinusoidal excitation; (e) 40 mm amplitude sinusoidal excitation; (f) wave elevation response amplitude for the 5 lateral excitation cases.

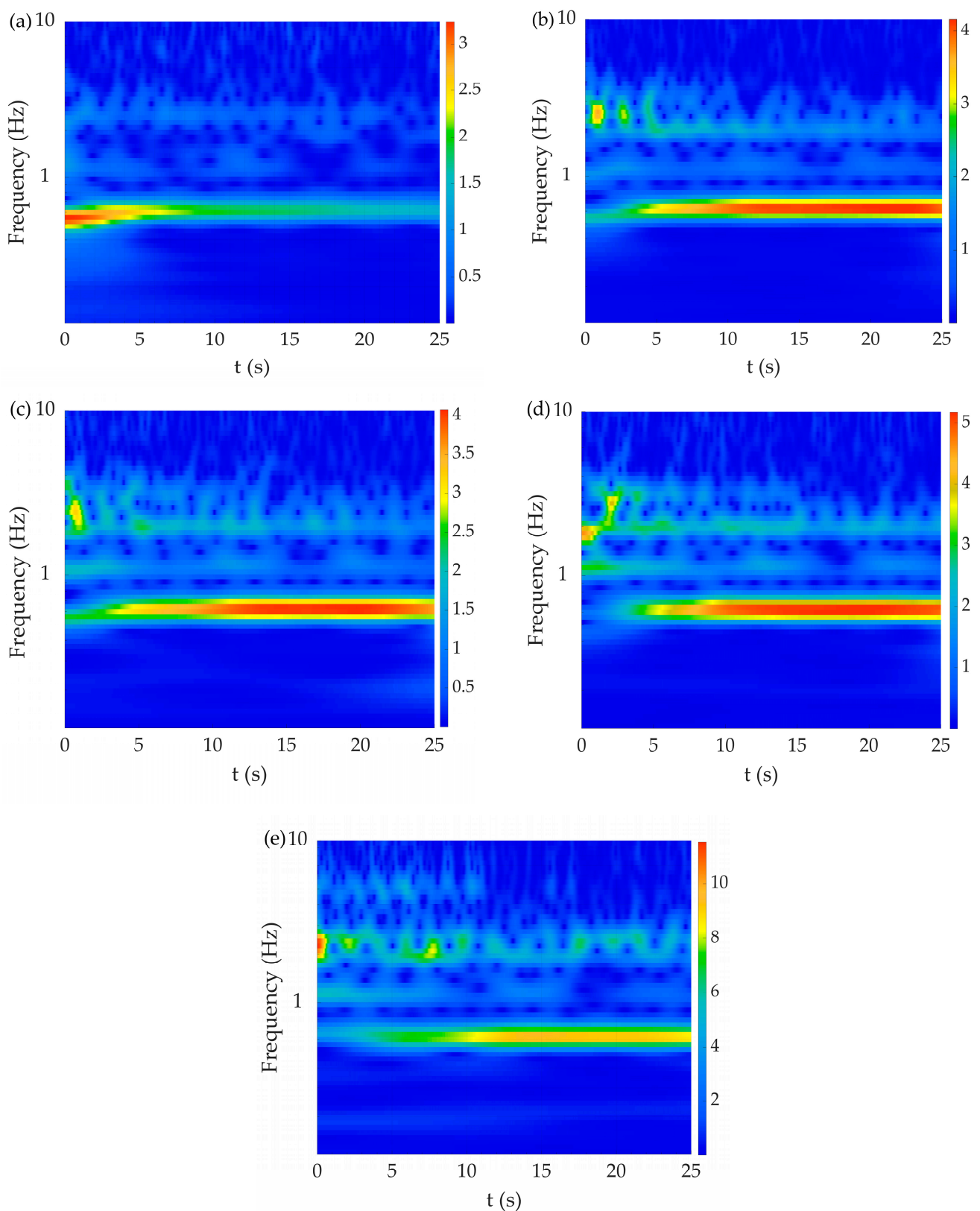


Figure 8. Wavelet scalograms of time histories of experimental wave elevation without band-pass filter: (a) 5 mm amplitude sinusoidal excitation; (b) 10 mm amplitude sinusoidal excitation; (c) 15 mm amplitude sinusoidal excitation; (d) 20 mm amplitude sinusoidal excitation; (e) 40 mm amplitude sinusoidal excitation. The color bar indicates the magnitude.

To evaluate the ability of the TLD system to dissipate energy, Figure 9 shows the decay part of the filtered time histories of wave elevation for two different excitation amplitudes. For a better presentation, only the decay part of the plots is shown. It is observed in Figure 9 that the TLD model is able to dissipate energy for the amplitudes of the considered excitation. Similar results were obtained for the rest of the amplitude excitations considered and for that reason they are not shown.

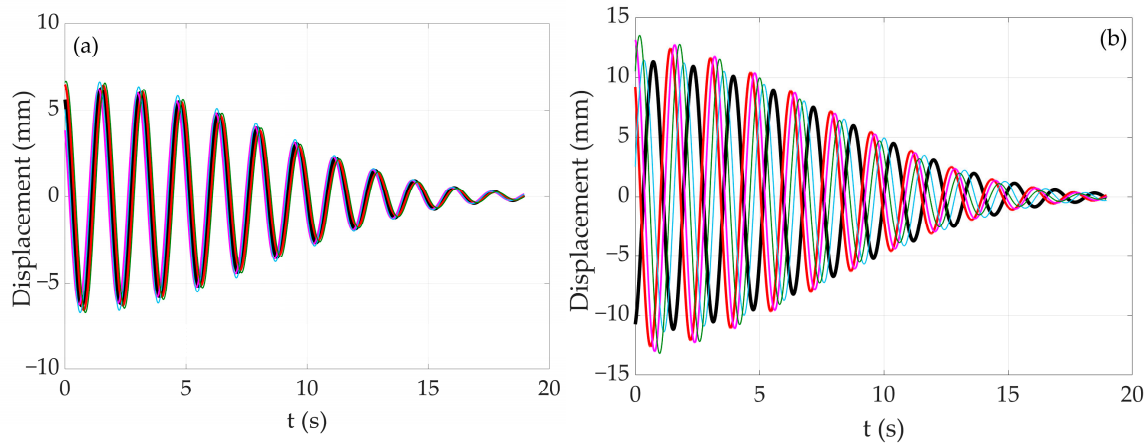


Figure 9. Time histories of free decay of the experimental wave height for different amplitudes: (a) 20 mm amplitude sinusoidal excitation; (b) 40 mm amplitude sinusoidal excitation. Time has been restarted from 0 for a better presentation of the decay part.

To identify the ratio of damping of the TLD (ζ_{TLD}), the traditional method of free-vibration decay was used. The filtered time histories of wave elevation were employed, with a total of 12 selected peaks to calculate ζ_{TLD} .

Table 3 shows the identified damping and frequency values for the 5 excitation amplitudes considered. The results presented in Table 3 correspond to the mean values of the 5 tests carried out for each excitation amplitude (see Table 2). It is observed from Table 3 that the mean values of the identified dynamic properties for the different amplitude values are very similar to the target values of 0.625 Hz, for the frequency, and 0.05 for damping. It is also observed from Table 3 that the error between the identified frequency and damping with respect to the target values ranges from 0.93 to 2.9%, and from 1.6 to 8.8%, respectively.

Table 3. Identified dynamic properties of the TLD model.

Excitation Amplitude A, mm	Frequency f_{w-exp} (Hz)	Frequency Error (%)	Damping ζ_{TLD}	Damping Error (%)
40	0.619	0.93	0.054	7.3
20	0.617	1.21	0.049	1.6
15	0.615	1.67	0.048	0.4
10	0.611	2.26	0.046	8.8
5	0.607	2.9	0.049	2.3

The experimental investigation included 25 tests where different excitation amplitudes were considered. Experimental tests with larger excitation amplitudes than those considered were not performed to avoid fluid spilling over the top of the tank. Excitation amplitudes of 15 mm and less cover the range of excitations that a TLD is expected to experience when placed over a structure subjected to wind excitation. Excitation amplitudes greater than 15 mm correspond to loads associated with seismic-induced response [34]. Figure 10 shows a summary of the results of each of the tests subjected to the different lateral demand amplitudes.

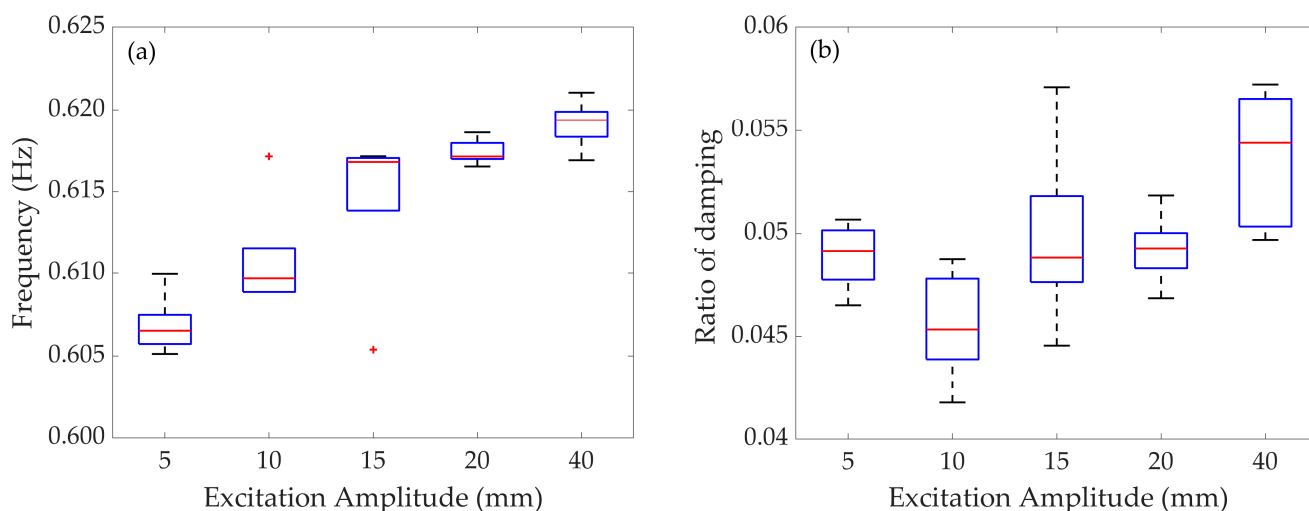


Figure 10. Influence of lateral demand amplitude variation on the identified dynamic properties of the TLD system: (a) Frequency; (b) Damping.

In Figure 10, the boxplots present statistics of the 5 frequency and damping samples calculated from the experimental data for different values of excitation amplitudes. For each boxplot, the median of the samples is indicated by a red line, the lower and upper limits of the box indicate the 25th and 75th percentiles, the most extreme data points not considered outliers are represented by whiskers, and outliers are represented individually using the cross symbol. It can be observed in Figure 10a that the dispersion of the identified frequencies is, in general, very similar along the amplitude of the excitation considered. It is also observed in Figure 10a an increasing trend of the identified frequencies along the amplitude of the excitation, which indicates that the identified frequency is closer to the target one for the greatest value of amplitude. It is also observed in Figure 10b, a greater dispersion of the data with respect to Figure 10a, and that no tendency is evident in the values of the damping ratio. Even though no clear tendency is observed in Figure 10b with respect to the amplitude of the excitation, the identified ratio of damping that is closer to the target one is associated with excitation amplitudes within 15 and 20 mm. The latter indicates that the employ of different amplitudes of the excitation during the tests is needed to improve the identification of parameters.

5. Conclusions

The experimental results to identify the dynamic properties of a TLD model using high-speed videos were presented. The identified dynamic properties of the TLD showed a good agreement with those employed for the design of the physical model, indicating that the use of high-speed videos can be a good alternative to evaluate the dynamic properties of TLD systems. The following specific conclusions are drawn:

- (1) The use of the program Tracker as a tool for high-speed video processing is a good option since its simple interface allows the user to generate time histories of displacements or accelerations with an acceptable level of error.
- (2) The use of bandpass filters to remove low- and high-frequency noise from the time histories extracted from Tracker improves the identification of parameters. In this study, a bandpass filter with corner frequencies equal to $0.95 f_w$ and $1.05 f_w$ was employed.
- (3) The procedure employed to evaluate the dynamic properties of a TLD system provided very good results. From the 25 experimental tests carried out, the identified dynamic properties for the different amplitude values are very similar to the target values, with errors between the identified frequency and damping with respect to the target values that range from 0.93 to 2.9% and 1.6 to 8.8%, respectively.

- (4) An increasing trend of the identified frequencies along the amplitude of the excitation was observed, indicating that the identified frequency is closer to the target one for the greatest value of amplitude (i.e., 40 mm).
- (5) No tendency is evident in the identified values of the damping ratio. Even though no clear tendency is observed, the identified ratio of damping that is closer to the target one is associated with excitation amplitudes within 15 and 20 mm.
- (6) The employ of different excitation amplitudes during the tests is needed to improve the identification of parameters.

It is worth mentioning that the experimental tests carried out in this work are not exhaustive, and only unidirectional lateral displacement of the sinusoidal type with amplitudes that range from 5 to 40 mm and frequency equal to 0.625 Hz were considered. Further experimental analyses that consider random displacement, not only in one direction but two, would be beneficial to evaluate the suitability of using high-speed videos to evaluate the dynamic properties and to study the main structure and TLD system in the context of hybrid simulation.

Author Contributions: Conceptualization, R.N.-G. and A.P.-E.; methodology, R.N.-G., A.P.-E. and O.P.-E.; investigation R.N.-G., A.P.-E., R.G.-M. and O.P.-E.; writing—original draft, R.N.-G., A.P.-E., R.G.-M. and O.P.-E.; writing—review and editing, A.P.-E. and R.G.-M.; resources, R.N.-G. and A.P.-E.; supervision, A.P.-E., R.G.-M. and O.P.-E. All authors have read and agreed to the published version of the manuscript.

Funding: This work was supported by UNAM-PAPIIT IN103422.

Data Availability Statement: The data presented in this study are available in the article.

Acknowledgments: The financial support of the National Council for the Humanities, Science and Technology (CONAHCYT) of Mexico and the Institute of Engineering are gratefully acknowledged. We thank Miguel Hernández and Osvaldo Martín del Campo for providing fruitful comments and suggestions to improve this work.

Conflicts of Interest: The authors declare no conflict of interest.

References

1. Li, J.; Wang, W. Seismic design of low-rise steel building frames with self-centering hybrid damping connections. *Resilient Cities Struct.* **2022**, *1*, 10–22. [[CrossRef](#)]
2. Yan, X.; Shu, G.; Rahgozar, N.; Alam, M. Seismic design and performance evaluation of hybrid braced frames having buckling-restrained braces and self-centering viscous energy-dissipative braces. *J. Constr. Steel Res.* **2024**, *213*, 108359. [[CrossRef](#)]
3. Konar, T.; Ghosh, A. A review on various configurations of the passive tuned liquid damper. *J. Vib. Control* **2023**, *9*, 1945–1980. [[CrossRef](#)]
4. Vandiver, J.K.; Mitome, S. Effect of liquid storage tanks on the dynamic response of offshore platforms. *Appl. Ocean. Res.* **1979**, *1*, 67–74. [[CrossRef](#)]
5. Kareem, A.; Sun, W. Stochastic response of structures with fluid-containing appendages. *J. Sound Vib.* **1987**, *119*, 389–408. [[CrossRef](#)]
6. Tamura, Y.; Fujii, K.; Ohtsuki, T.; Wakahara, T.; Kohsaka, R. Effectiveness of tuned liquid dampers under wind excitation. *Eng. Struct.* **1995**, *17*, 609–621. [[CrossRef](#)]
7. Housner, G.; Bergman, L.; Caughey, T.; Chassiakaros, A.; Claus, R.; Masri, S.; Skelton, R.E.; Soong, T.T.; Spencer, B.F.; Yao, J.T. Structural control: Past, present and future. *J. Eng. Mech.* **1997**, *123*, 897–971. [[CrossRef](#)]
8. Ren, H.; Fan, Q.; Lu, Z. Shaking table test and parameter analysis on vibration control of a new damping system. *Buildings* **2022**, *12*, 896. [[CrossRef](#)]
9. Poguluri, S.; Cho, I. Liquid sloshing in a rectangular tank with vertical slotted porous screen: Based on analytical, numerical and experimental approach. *Eng. Struct.* **2022**, *189*, 106373. [[CrossRef](#)]
10. Zhang, Z. Understanding and exploiting the nonlinear behavior of tuned liquid dampers (TLDs) for structural vibration control by means of a nonlinear reduced-order model (ROM). *Eng. Struct.* **2022**, *251*, 113524. [[CrossRef](#)]
11. Salaas, B.; Bekdas, G.; Ibrahim, Y.E.; Nigdeli, S.; Ezzat, M.; Nawar, M.; Kayabekir, A. Design optimization of a hybrid vibration control system for buildings. *Buildings* **2023**, *13*, 934. [[CrossRef](#)]
12. Tait, M. Modelling and preliminary design of a structure-TLD system. *Eng. Struct.* **2008**, *30*, 2644–2655. [[CrossRef](#)]
13. Altay, O. *Vibration Mitigation Systems in Structural Engineering*, 1st ed.; CRC Press: Boca Raton, FL, USA, 2021.

14. Tait, M.; El Damatty, A.; Isyumov, N.; Siddique, M. Numerical flow models to simulate tuned liquid dampers (TLD) with slat screens. *J. Fluids Struct.* **2005**, *20*, 1007–1023. [[CrossRef](#)]
15. Hamelin, J.; Love, J.; Tait, M.; Wilson, J. Tuned liquid dampers with Keulegan-Carpenter number-dependent screen drag coefficient. *J. Fluids Struct.* **2013**, *43*, 271–286. [[CrossRef](#)]
16. Ruiz, R.; López-García, D.; Taflanidis, A. Modeling and experimental validation of a new type of tuned liquid damper. *Acta Mech.* **2016**, *227*, 3275–3294. [[CrossRef](#)]
17. Konar, T.; Ghosh, A. Flow damping devices in tuned liquid damper for structural vibration control: A review. *Arch. Comput. Methods Eng.* **2021**, *28*, 2195–2207. [[CrossRef](#)]
18. Konar, T.; Ghosh, A. Development of a novel tuned liquid damper with floating base for converting deep tanks into effective vibration control devices. *Adv. Struct. Eng.* **2021**, *24*, 401–407. [[CrossRef](#)]
19. Love, J.; Tait, M. A preliminary design method for tuned liquid dampers conforming to space restrictions. *Eng. Struct.* **2012**, *40*, 187–197. [[CrossRef](#)]
20. Love, J.; Morava, B.; Robinson, J.; Haskett, T. Tuned sloshing dampers in tall buildings: A practical performance-based design approach. *Pract. Period. Struct. Des. Constr.* **2021**, *26*, 04021016. [[CrossRef](#)]
21. Porrás, R.; Mobaraki, B.; Lozano-Galant, J.; Sanchez-Cambronero, S.; Prieto, F.; Gutierrez, J. New image recognition technique for intuitive understanding in class of the dynamic response of high-rise buildings. *Sustainability* **2021**, *13*, 3695. [[CrossRef](#)]
22. Pozos-Estrada, O.; Rojas-Flores, M.; Avalos-Saucedo, F.; Avila-Lopez, S. Experimental investigation of air concentration profiles in a dam bottom outlet by using gray scale images with high resolution. *J. Vis.* **2022**, *25*, 1189–1207. [[CrossRef](#)]
23. Gandarson, M. Shallow-Water Sloshing. Ph.D. Thesis, University of Washington, Seattle, WA, USA, 1997.
24. Lobovský, L.; Botia-Vera, E.; Castellana, F.; Mas-Soler, J.; Souto-Iglesias, A. Experimental investigation of dynamic pressure loads during dam break. *J. Fluids Struct.* **2014**, *48*, 407–434. [[CrossRef](#)]
25. Min, K.; Jang, S.; Kim, J. A standalone vision sensing system for Pseudodynamic testing of tuned liquid column dampers. *J. Sens.* **2016**, *2016*, 8152651. [[CrossRef](#)]
26. Poguluri, S.; Cho, I. Mitigation of liquid sloshing a rectangular tank due to slotted porous screen. *J. Eng. Marit. Environ.* **2020**, *234*, 686–698. [[CrossRef](#)]
27. Xu, B.; Han, Z.; Wang, L.; Liu, Q.; Xu, X.; Chen, H. The influence of integral water tank on the seismic performance of slender structure: An experimental study. *Buildings* **2023**, *13*, 736. [[CrossRef](#)]
28. Xiao, C.; Wu, Z.; Chen, K.; Tang, Y.; Yan, Y. Development of a water supplement system for tuned liquid damper under excitation. *Buildings* **2023**, *13*, 1115. [[CrossRef](#)]
29. Nava-González, R. Comparison of Wind Effects in a Slender Building: Analytical Methodology vs Experimental Methodology in Wind Tunnel. Master's Thesis, National Autonomous University of Mexico, Mexico City, Mexico, 2019.
30. Ibrahim, R. *Liquid Sloshing Dynamics: Theory and Applications*, 1st ed.; Cambridge University Press: Cambridge, UK, 2005.
31. Tait, M.; El Damatty, A.; Isyumov, N. An investigation of tuned liquid dampers equipped with damping screens under 2D excitation. *Earthq. Eng. Struct. Dyn.* **2005**, *34*, 719–735. [[CrossRef](#)]
32. Brown, D. Tracker Video Analysis and Modelling Tool, Open Source Physics [Computer Software]. Available online: <https://physlets.org/tracker/> (accessed on 1 January 2023).
33. Chopra, A. *Dynamics of Structures*, 5th ed.; Pearson: Jacksonville, FL, USA, 2016.
34. Love, J.; Tait, M. Parametric depth ratio study on tuned liquid dampers: Fluid modelling and experimental work. *Comput. Fluids.* **2013**, *79*, 13–26. [[CrossRef](#)]

Disclaimer/Publisher's Note: The statements, opinions and data contained in all publications are solely those of the individual author(s) and contributor(s) and not of MDPI and/or the editor(s). MDPI and/or the editor(s) disclaim responsibility for any injury to people or property resulting from any ideas, methods, instructions or products referred to in the content.